Animal Study

SIRT1 Facilitates Beclin-1 Nuclear Translocation to Mitigate Nociceptive Hypersensitivity in Rats with Bone Cancer Pain by Restoring Autophagic Flux

Qiuli He, MD[1], Wenjie Li, MB[2], Cuie Deng, MB[3], Zhiming Zhang, MD[2], and Housheng Deng, MD[2]

From: [1]Department of Anesthesiology and Pain Research Center, Jiaxing University Affiliated Hospital, The First Hospital of Jiaxing, Jiaxing, Zhejiang Province, China; [2]Department of Anesthesiology, Chenzhou NO.1 People's Hospital, Chenzhou, Hunan Province, China; [3]School of Public Health, Shenyang Medical College, Shenyang, Liaoning Province, China

Address Correspondence: Housheng Deng Department of Anesthesiology, Chenzhou NO.1 People's Hospital, Chenzhou, Hunan Province, China E-mail: 15601620846@163.com

Disclaimer: This study was supported by grants from the Natural Science Foundation of Zhejiang Province (LTGD23H090003), the Jiaxing Public Welfare Research Project (2022AY10017), and the Natural Science Foundation of Hunan Province (2026JJ80594).

Conflict of interest: Each author certifies that he or she, or a member of his or her immediate family, has no commercial association (i.e., consultancies, stock ownership, equity interest, patent/licensing arrangements, etc.) that might pose a conflict of interest in connection with the submitted article.

Article received: 03-13-2025
Revised article received: 06-20-2025
Accepted for publication: 08-08-2025

Free full article: www.painphysicianjournal.com

Background: The etiology of bone cancer pain (BCP) is multifaceted, and effective therapeutic strategies for treating the condition remain elusive. Prior research has implicated sirtuin 1 (SIRT1) in the pathogenesis of BCP, suggesting the protein's potential to modulate autophagy and mitigate nociceptive sensitization; however, the underlying mechanisms of BCP are not fully understood.

Objectives: This study aimed to elucidate the role of SIRT1 in activating autophagy and its impact on the development of nociceptive hypersensitivity in a rat model of BCP.

Study Design: Controlled animal study.

Setting: Female Sprague Dawley® rats weighing 180–220 g were used.

Methods: The BCP model was established by a single injection of Walker 256 breast cancer cells (10 μL, 10^7cells/mL) into the tibia. Mechanical pain sensitivity was assessed behaviorally using an Electronic von Frey Anesthesiometer.

Results: Western blot (WB) analysis revealed reduced SIRT1 levels and elevated beclin-1 expression, an increased LC3II/LC3I ratio, and enhanced P62 expression in the dorsal horns of spinal cord tissues from rats with BCP. Immunofluorescence assays demonstrated co-localization of SIRT1 with neuronal cells and beclin-1. Subsequent experiments indicated that intrathecal administration of a SIRT1 agonist in rats with BCP postponed the downregulation of SIRT1, decreased the acetylation of beclin-1, and facilitated beclin-1 nuclear translocation. This treatment also led to a reduction in the LC3II/LC3I ratio and P62 expression levels. Collectively, these findings suggest that SIRT1 may ameliorate nociceptive hypersensitivity in rats with BCP through the promotion of beclin-1 nuclear translocation, thereby restoring autophagic flux.

Limitations: This study focused on peripheral/spinal mechanisms but not supraspinal/cortical contributions. Pharmacological tests were limited to a single time point, potentially missing dynamic pain changes during tumor progression. Nevertheless, the findings of this study offer valuable preliminary insights.

Conclusion: This research uncovers a novel mechanism of SIRT1 in the genesis of nociceptive hypersensitivity in BCP and offers potential avenues for therapeutic intervention.

Key words: SIRT1, beclin-1, autophagic flux, bone cancer pain

Pain Physician 2026: 29:E55-E69

Bone cancer pain (BCP) commonly affects patients with advanced breast, prostate, and lung cancers due to frequent skeletal metastases (1). Although sometimes asymptomatic, bone metastases often cause severe complications, including fractures, hypercalcemia, and spinal cord compression, impairing patients' quality of life and chances of survival significantly (2-4). Current understanding of cancer-induced pain mechanisms remains limited, leading to suboptimal clinical management. BCP's dual neuropathic-inflammatory nature involves peripheral tissue alterations, nerve fiber changes, and neurochemical adaptations across neural levels (5,6). Elucidating these complex mechanisms is critical for improving pain management.

Sirtuin 1 (SIRT1), an NAD^+-dependent deacetylase, regulates diverse biological processes through protein deacetylation, enabling rapid gene expression adjustments to environmental stimuli (7). Emerging evidence positions SIRT1 as a therapeutic target for chronic pain (8). Research has indicated that SIRT1 can serve as a therapeutic target in the management of chronic pain (8). In a rat model of BCP, intrathecal administration of SRT1720, an activator of SIRT1, has been shown to alleviate pain by suppressing mitochondrial fission mediated by dynamin-related protein 1 (Drp1) (9). Similarly, the activation of SIRT1 has been reported to diminish BCP by inhibiting the activation of metabotropic glutamate receptors (mGluRs), specifically mGluR1 and mGluR5 (mGluR1/5) (10). Furthermore, a study utilizing a mouse model of BCP demonstrated that intrathecal melatonin injections mitigated pain by curbing HMGB1 nuclear translocation and the release of inflammatory cytokines through SIRT1-mediated pathways (11). Despite these findings, the precise role of SIRT1 in the etiology of BCP warrants further elucidation. Evidence suggests that SIRT1 may ameliorate pain by modulating autophagy, a hypothesis that merits deeper exploration (12,13).

Autophagy maintains cellular homeostasis by degrading dysfunctional components. Beclin-1, a pivotal autophagy regulator, governs autophagosome membrane formation and modulates autophagic flux (14-16). The nuclear translocation of Beclin-1 may influence autophagosome assembly (17), with proposed roles in cellular functions like endometrial remodeling (17). However, conflicting research indicates that Beclin-1 nuclear translocation does not regulate autophagy directly and participates in DNA repair independently (18), suggesting potential indirect links between nuclear functions and autophagy. Critically, Beclin-1 activation mitigates nociceptive hypersensitivity by enhancing autophagic flux in pain models (19-21), supporting the therapeutic potential of autophagy. SIRT1 may exert therapeutic effects via autophagy activation (22,23), but the protein's role in promoting Beclin-1 nuclear translocation and autophagic flux for pain relief remains undetermined, with the underlying mechanisms unclear.

In this study, using a rat BCP model, we investigated SIRT1 expression dynamics, Beclin-1 nuclear translocation, and autophagic flux modulation. The aim was to elucidate how the activation of a SIRT1/autophagy pathway mitigates nociceptive hypersensitivity, thereby clarifying SIRT1's role in BCP pathogenesis and identifying novel therapeutic strategies.

Methods

Study Design

Adult female Sprague-Dawley® (SD) rats, weighing between 180-220 grams, were sourced from Shanghai Legian Biotechnology Co., Ltd. These animals had ad libitum access to food and water throughout the study. Rats were divided into a sham group, a BCP group, an SRT1720 group, and an EX527 group, intrathecally injected with a SIRT1 activator or inhibitor, and then used to explore the role of SIRT1 in the development of BCP. All animal experiments and associated protocols were conducted in strict accordance with the guidelines set by the Institutional Animal Care and Use Committee (IACUC) of Jiaxing University, and prior approval was obtained from this committee.

Tumor Cell Preparation

The methodology for preparing tumor cells has been detailed in previous studies by Mao-Ying et al (24). In this experiment, Walker-256 breast cancer cells were administered intraperitoneally to female rats. Following a one-week incubation period, the cancer cells were harvested and promptly washed with phosphate-buffered saline (PBS) solution to remove any contaminants. Subsequently, these cells were resuspended to achieve a final concentration of 10^7 cells/mL. For the sham operation group, an equivalent concentration of heat-killed cancer cells was utilized to control for non-specific effects.

Establishment of Rat Model of BCP

Adult female SD rats were utilized in this study. Anesthesia was induced via intraperitoneal injection

of sodium pentobarbital at a dosage of 60 mg/kg. Following anesthesia, an epidermal incision was made on the left leg, allowing exposure of the lower third of the tibia. A small hole was drilled into the tibial shaft, and either Walker-256 tumor cells (at a concentration of 10^7 cells/mL) or heat-killed cells were injected into the bone cavity. The syringe was retained in situ for approximately one minute to prevent the injected material from leaking. After the injection, the syringe was removed, and the puncture site was sealed with bone wax and sutured. The incision was then dressed with gentamycin ophthalmic ointment to prevent infection. Rats were subsequently placed on a heating pad to facilitate natural recovery from anesthesia. To evaluate the proliferation of tumor cells within the intramedullary space of the tibia, computed tomography (CT) radiography was employed.

Intrathecal Drug Delivery

Adult female SD rats were briefly anesthetized using intraperitoneal injection of sodium pentobarbital at a dosage of 50 mg/kg. Following the administration of anesthesia and the shaving of each rat's dorsal region, a PE-10 catheter was carefully inserted through the intervertebral disc into the subarachnoid space. The microtubule was then anchored securely to the adjacent ligament, ensuring that the free end of the microtubule extended 2 cm beyond the anchor point. This free end was exposed and then capped to prevent contamination, and the surgical incision was meticulously closed. On the second day after surgery, the efficacy of the catheter placement was confirmed by the induction of paralysis in both hind limbs following the injection of 10 µl of lidocaine along the catheter. Intrathecal catheterization was performed immediately after the model preparation, with drug administration commencing 6 days postoperatively and continuing for a total of 12 days after the operation.

Paw Withdrawal Threshold Measurement

Paw withdrawal threshold (PWT) measurements for the left hind paw were conducted using the Electronic von Frey Anesthesiometer (IITC Life Science, Inc.). Before each testing session, rats were allowed to acclimate individually in a Plexiglas chamber (25 × 20 × 20 cm) for 30 minutes on a wire mesh platform. The PWT test was performed 3 times, with a minimum interval of 5 minutes between successive stimuli. PWT values, expressed in grams, represented the maximum tolerable force and were calculated as the average of the 3 measurements. All behavioral assessments were carried out by investigators who were blinded to the experimental group assignments.

Primary Culture of Neuronal Cells

Neonate rat spinal cords were used for primary neuronal culture. After removing membranes and blood vessels, the cords were dissected into one-cm^3 pieces. These were digested with 0.05% trypsin at 37°C for 15-20 minutes, with agitation every 5 minutes. Trypsin was inactivated with an inhibitor, and the mixture was pipetted to create a suspension. The cells were centrifuged at 1000 rpm at 4°C for 10 minutes, and the pellet was resuspended in the first planting solution. Differential adhesion was performed in a culture flask at 37°C, 5% CO_2, and 95% humidity for 30 minutes. The supernatant, rich in neurons, was collected, and cell counts were determined using trypan blue staining. Cells were seeded into 6-well plates at 6×105 cells per well and incubated under the same conditions. On day 2, the medium was refreshed with planting solution 2. On day 4, 5 µM cytarabine was added for a partial exchange, followed by a full exchange after 24 hours. The medium was then changed twice weekly to maintain optimal conditions.

Hematoxylin-Eosin Staining

On day 12 after tumor inoculation, rats were deeply anesthetized with a lethal dose of pentobarbital (80 mg/kg, intravenously) and subsequently euthanized. Tibial tissue, approximately one cm in length surrounding the inoculation site, was harvested and decalcified in a 10% EDTA solution for a duration of 24 hours. Following decalcification, the tissue underwent dehydration and was embedded in paraffin. Sections of the embedded tissue, 8 µm thick, were prepared using a rotary microtome. These sections were then stained with hematoxylin and eosin (H-E) to assess tumor cell infiltration, tumor size, and the degree of bone destruction. Examination of the stained sections was conducted using a microscope (Olympus BX51) with 10× or 20× objective lenses to visualize the histological details.

CT Bone Reconstruction Examination

To ascertain the degree of tibial bone destruction induced by tumor inoculation, bone reconstruction was conducted via CT on the left tibial bones of the rats on the twelfth day after the cancer-cell inoculation. The rats were anesthetized with an overdose of pentobarbital (60 mg/kg, intravenously) prior to the

procedure and then euthanized. The intraosseous bone was assessed using an E-COM technology digital radiography system, recognized for its advanced imaging capabilities and optimal image quality with lower doses of radiation.

Immunofluorescence

Twelve days after the surgery, rats were anesthetized deeply with intravenous pentobarbital (80 mg/kg) and then perfused intracardially with 4% phosphate-buffered paraformaldehyde. The lumbar-expanded tissues were rapidly excised and fixed in the aforementioned fixative solution for 4-6 hours. Subsequently, the tissues were dehydrated in a gradient of sucrose (10%-30%) in sterile water over 5-7 days at 4°C, followed by a 2-hour incubation in optimal cutting temperature (OCT) compound at 4°C. The tissues were embedded in OCT compound (Sakura Finetek) and frozen at -25°C in a cryostat. Serial sections, 25 μm thick, were prepared and mounted onto microscope slides (CITOGLAS®, CITOTEST). The sections were blocked with 10% goat serum and 0.03% Triton X-100 in PBS for one hour at room temperature. Those sections were then incubated overnight at 4°C with a mixture containing 10% goat serum and primary antibodies. The primary antibodies used were rabbit anti-SIRT1 (ab110304, 1:1000, Abcam Limited), mouse anti-Beclin-1 (bsm-33315M, 1:400, Bioss USA), rabbit anti-LC3 (4108S, 1:1000, Cell Signaling Technology [CST]), rabbit anti-P62 (23214, 1:1000, CST), mouse anti-NeuN (ab104224, 1:1000, Abcam), mouse anti-Iba1 (ab283319, 1:500, Abcam), and mouse anti-GFAP (ab10062, 1:300, Abcam). For immunofluorescence, sections were incubated with Alexa Fluor® 594 goat anti-rabbit IgG (ab150064, 1:1000, Abcam) and Alexa Fluor® 488 goat anti-mouse IgG (ab150113, 1:1000, Abcam) for one hour at 25°C, followed by counterstaining with DAPI (HNFD-02, 5μl, HelixGen). For immunohistochemical staining, sections were incubated with horseradish peroxidase (HRP)–conjugated rabbit anti-mouse IgG secondary antibody (1:200, Abcam) for one hour at 25°C. Positive staining was visualized using a DAB peroxidase substrate kit, and sections were counterstained with hematoxylin. Images from the dorsal horn of the spinal cord were captured using a confocal microscope (TCS SP2, Leica Microsystems) or an optical microscope. Measurements and analyses were conducted using Image-Pro Plus 6.0 software (Media Cybernetics, Inc.). A total of 9-16 images from 4 rats per group, with 24 sections per sample, were collected and analyzed.

Immunoblotting

On day 12 after tumor inoculation, the rats were deeply anesthetized with a lethal dose of intravenous pentobarbital (80 mg/kg) and euthanized. The L3-L5 segments of the rats' spinal cords were rapidly harvested and preserved in liquid nitrogen. Tissue homogenates were prepared and subjected to cytoplasmic extraction using a radioimmunoprecipitation assay (RIPA) buffer (Sigma-Aldrich). The homogenates were centrifuged at 13,000 rpm for 10 minutes at 4°C to separate the supernatant. The protein concentration of the supernatant was quantified using the bicinchoninic acid (BCA) assay. For co-immunoprecipitation (co-IP), 500 μL of the supernatant was incubated with one μg of the appropriate primary antibody at 4°C overnight with gentle agitation. The next day, 20 μL of protein A/G agarose beads were added and incubated for 2-4 hours at 4°C with continued agitation. The mixture was then centrifuged at 3,000 rpm for 3 minutes to pellet the beads. The supernatant was carefully removed, and the beads were washed 3 times with 1 mL of the cold RIPA buffer. After the final wash, the beads were resuspended in 60 μL of 2x SDS-PAGE loading buffer, boiled for 5 minutes to dissociate the protein-antibody complexes, and centrifuged to collect the supernatant for further analysis. For the WB analysis, equal amounts of protein (50 μg) from each sample were resolved by Tris-Tricine SDS-PAGE (10%) and transferred onto nitrocellulose membranes (Sigma). The membranes were blocked for one hour at 25°C then incubated with the appropriate primary antibodies for 6-8 hours at 4°C, followed by detection with HRP-conjugated secondary antibodies. The primary antibodies used were rabbit anti-SIRT1 (ab110304, 1:1000, Abcam), rabbit anti-Beclin-1 (#3738, 1:500, CST), rabbit anti-Pan Acetyl-Lysine (#3738, 1:500, Abclonal), rabbit anti-Rabbit pAb (#3738, 1:500, Abclonal), rabbit anti-LC3 (4108S, 1:2000, CST), and rabbit anti-P62 (sc-8393, 1:500, Santa Cruz Biotechnology). The blots were developed using a chemiluminescent HRP substrate (Millipore). Band intensities were analyzed using Quantity One® software (Bio-Rad Laboratories), normalized to β-actin levels, and expressed as a percentage relative to the control group.

Statistical Analysis

All data are presented as the mean ± SD and were analyzed using IBM SPSS Statistics 24.0 (IBM Corporation). To assess differences in molecular expression levels or behavioral scores among groups, one-way or 2-way analysis of variance (ANOVA) was employed, fol-

lowed by post hoc Bonferroni correction, as appropriate. Statistical significance was determined at the $P < 0.05$ level.

Results

The BCP Rat Model Was Established Successfully

In the BCP model, there was a notable reduction in PWT values from 6 to 18 days after surgery, as depicted in Fig. 1A. Three-dimensional reconstruction of the tibia revealed extensive bone destruction in BCP rats, which was further confirmed by hematoxylin and eosin (H&E) staining, showing significant trabecular fractures and tumor infiltration in BCP rats, in contrast to the absence of bone destruction in sham-operated rats, as illustrated in Fig. 1C. Gait analysis also demonstrated that the left hind paw of rats in the BCP group exhibited a significantly reduced maximal touch area, maximal touch strength, and mean touch strength compared to the sham group, as shown in Figs. 1D-H. Rats inoculated with heat-killed cells did not display pain-related behaviors, as indicated in Fig. 1A. Collectively, these findings confirm the successful establishment of a rat model of BCP in the present study.

In BCP Rats, Expression of SIRT1 Is Low and Expression of Beclin-1 Is High

Previous studies have shown that the expression of SIRT1 in chronic pain models is low (8). In addition, numerous studies have indicated that enhancing autophagy may activate neuronal signaling to alleviate pain hypersensitivity during the development of the pain condition (14,25). Thus, the current study investigated the alterations in the expression levels and cellular distribution of SIRT1 and Beclin-1 within a successfully established rat model of BCP. WB analysis revealed that SIRT1 expression was markedly reduced, whereas Beclin-1 expression was significantly elevated in the BCP rats at 12 days after modeling as compared to the sham group (Figs. 2A-C). Furthermore, immunofluorescence assays demonstrated that SIRT1 was co-localized with spinal cord neurons, with no significant co-localization observed with microglia or astrocytes (Fig. 2D). Concurrently, immunofluorescence double-labeling indicated a co-localization of SIRT1 with Beclin-1 (Fig. 2E).

Impaired Autophagy Flux in BCP Rats

LC3 and p62 are key proteins in the autophagy process, and by detecting the changes in the LC3-II/I ratio and the expression level of p62, the level of autophagy can be assessed (26). To further detect the changes in autophagy activity in rats with BCP, WB analysis revealed that autophagy markers within the BCP group were significantly different from those in the sham group. Specifically, the ratio of LC3II to LC3I was markedly elevated, indicating an accumulation of autophagosomes, and the expression levels of P62 were also increased, suggesting impaired autophagic flux (Figs. 3A-C). Additionally, immunofluorescence studies demonstrated that LC3 co-localized with neuronal cells (Fig. 3D), and a similar co-localization pattern was observed for P62 (Fig. 3E). Collectively, these findings suggest that disruptions in neuronal autophagy may play a role in the development of nociceptive sensitization associated with BCP and that this process may possibly be regulated by SIRT1.

SIRT1 Plays a Role in the Development of Nociceptive Hypersensitivity in Rats with BCP

Subsequently, to investigate the role of SIRT1 in BCP hypersensitivity, this study evaluated the impact of the SIRT1 agonist SRT1720 and the inhibitor EX527 via intrathecal injection. Behavioral assays demonstrated that, in comparison to the BCP group, rats treated with SRT1720 exhibited a statistically significant enhancement in hind PWT on days 9, 12, 15, and 18 after the modeling. Conversely, also in comparison to the BCP group, rats treated with EX527 displayed a statistically significant reduction in hind PWT on days 9 and 12 after the modeling; no significant differences in PWT were observed at other time points (Fig. 4A). WB analysis further revealed that SIRT1 expression was significantly higher in the SRT1720 group than in the BCP group, as was Beclin-1 expression. In contrast, rats in the EX527 group showed a significant decrease in SIRT1 expression at 12 days after the modeling, along with a corresponding decrease in Beclin-1 expression (Figs. 4B-D). These findings suggest that SIRT1 may mitigate the development of nociceptive hypersensitivity in BCP rats, potentially through its regulation of Beclin-1 expression.

SIRT1 Facilitates Beclin-1 Nuclear Translocation, Thereby Enhancing Autophagy Flux

While Beclin-1 is a key protein in the autophagy process, it is widely recognized that this protein's localization in the cytosol is essential for its significant role in autophagy (27). Building on this observation, the

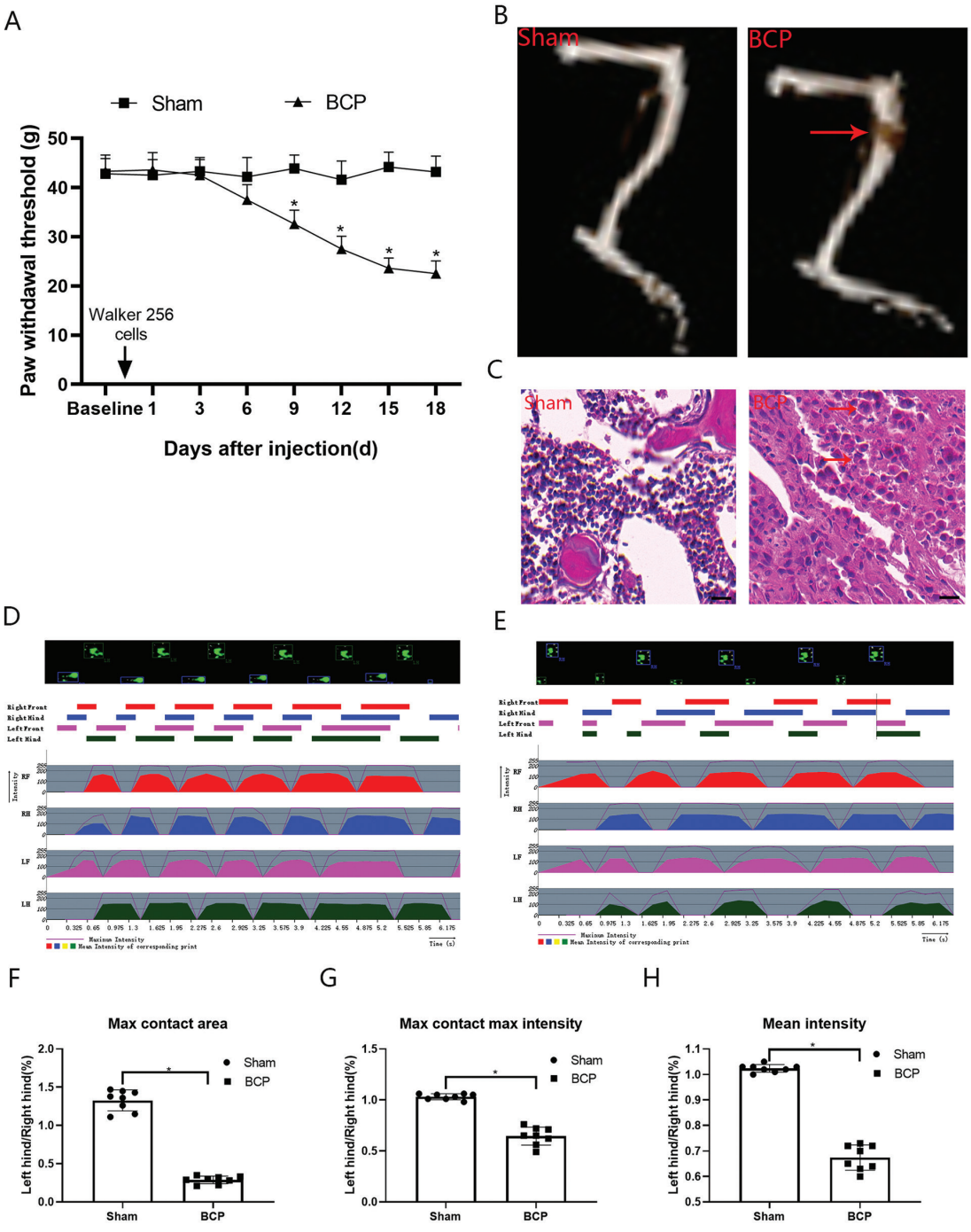

Fig. 1. *Establishment and characterization of a rat bone cancer pain (BCP) model. (A) A significant reduction in paw withdrawal threshold (PWT) post-surgery (n = 12). (B) Three-dimensional reconstruction of the tibia, revealing extensive bone destruction in BCP rats at 12 days after inoculation, indicated by red arrows. (C) Hematoxylin and eosin (H&E) staining of tibial sections, demonstrating malignant tumor infiltration in BCP rats at 12 days after inoculation, as marked by the red arrow. (D-H) Gait analysis in rats, showing a decrease in maximal touch area, maximal touch strength, and mean touch strength of the hind paw in the BCP pain group compared to the sham group. For behavioral and molecular analyses, statistical significance was determined at *P < 0.05 versus the sham group, using one-way ANOVA followed by Bonferroni post-hoc test.*
Abbreviations: BCP, bone cancer pain; PWT, paw withdrawal threshold.

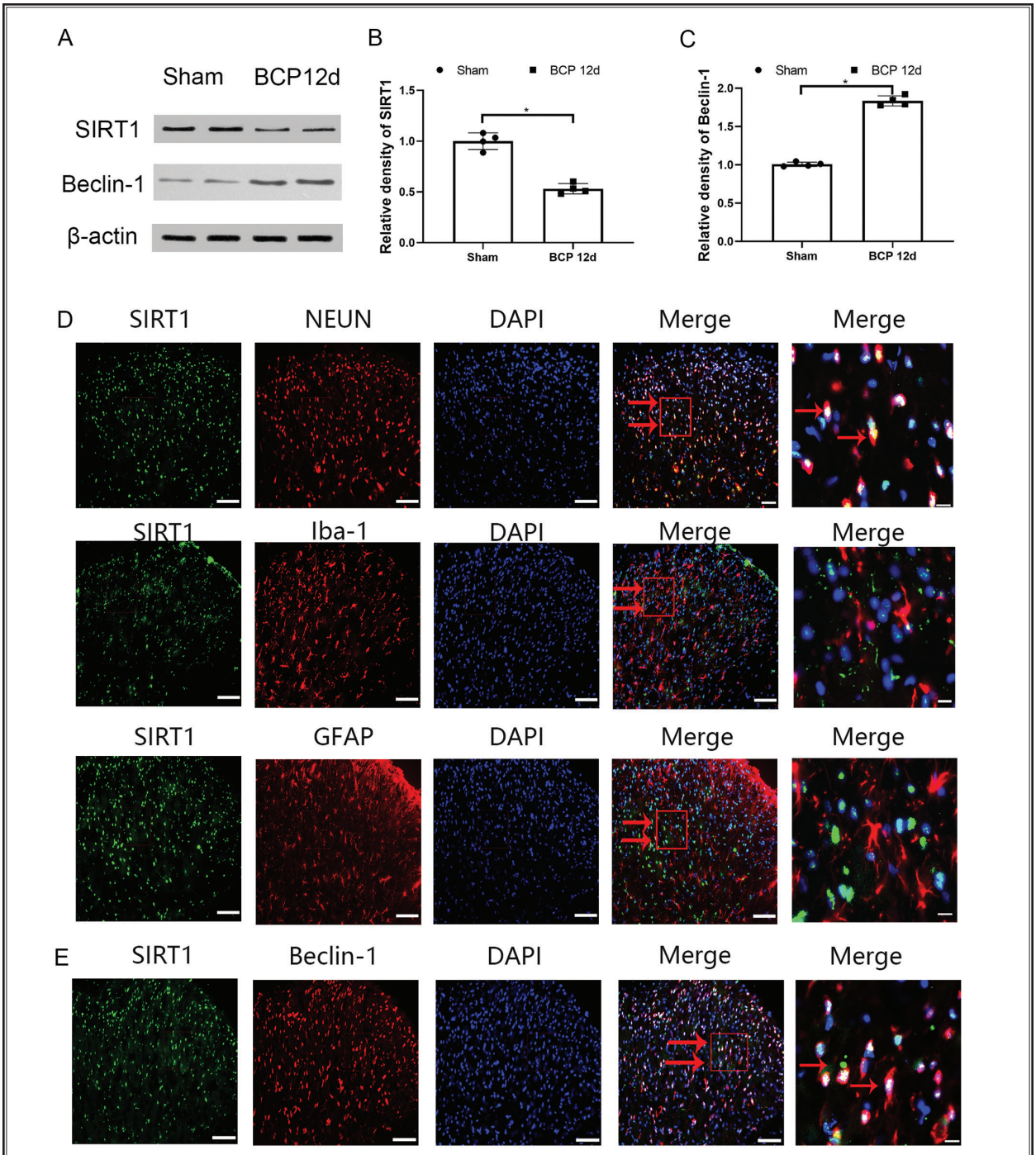

Fig. 2. *Expression and cellular localization of SIRT1 and Beclin-1.*
*(A-C) Western blot analysis reveals alterations in the expression levels of SIRT1 and Beclin-1 in the spinal cord tissue of BCP rats compared to the sham group (n = 4). (D) Immunofluorescence double labeling demonstrates the cellular distribution of SIRT1, which is co-localized with spinal cord neurons (indicated by red arrows) but not with microglia or astrocytes (n = 4). (E) Co-localization of SIRT1 with Beclin-1 is observed, as marked by red arrowheads (n = 4). Statistical significance was determined at *P < 0.05 versus the sham group, using one-way ANOVA followed by a Bonferroni post-hoc test. The scale bar represents 25 or 50 μm.*

study delved into the regulatory role of SIRT1 on Beclin-1 in the context of BCP. Co-IP assays revealed that the expression levels of acetylated Beclin-1 were significantly lower in rats treated with the SIRT1 agonist SRT1720 than in the BCP group, and the difference was statistically significant. Conversely, rats treated with the SIRT1 inhibitor EX527 exhibited a significant increase in acetylated Beclin-1 levels (Figs. 5A-B). Immunofluorescence assays further demonstrated an enhanced nuclear translocation of Beclin-1 in the SRT1720 group relative to the BCP group (Fig. 5C). WB analysis results indicated that rats in the SRT1720 group experienced a statistically significant reduction in LC3II/LC3I ratio and P62 expression when compared to the BCP group. In contrast, rats in the EX527 group showed an increase in LC3II/LC3I ratio and P62 expression, both with statistically significant differences from the BCP group (Figs. 5D-F). Collectively, these results suggest that the

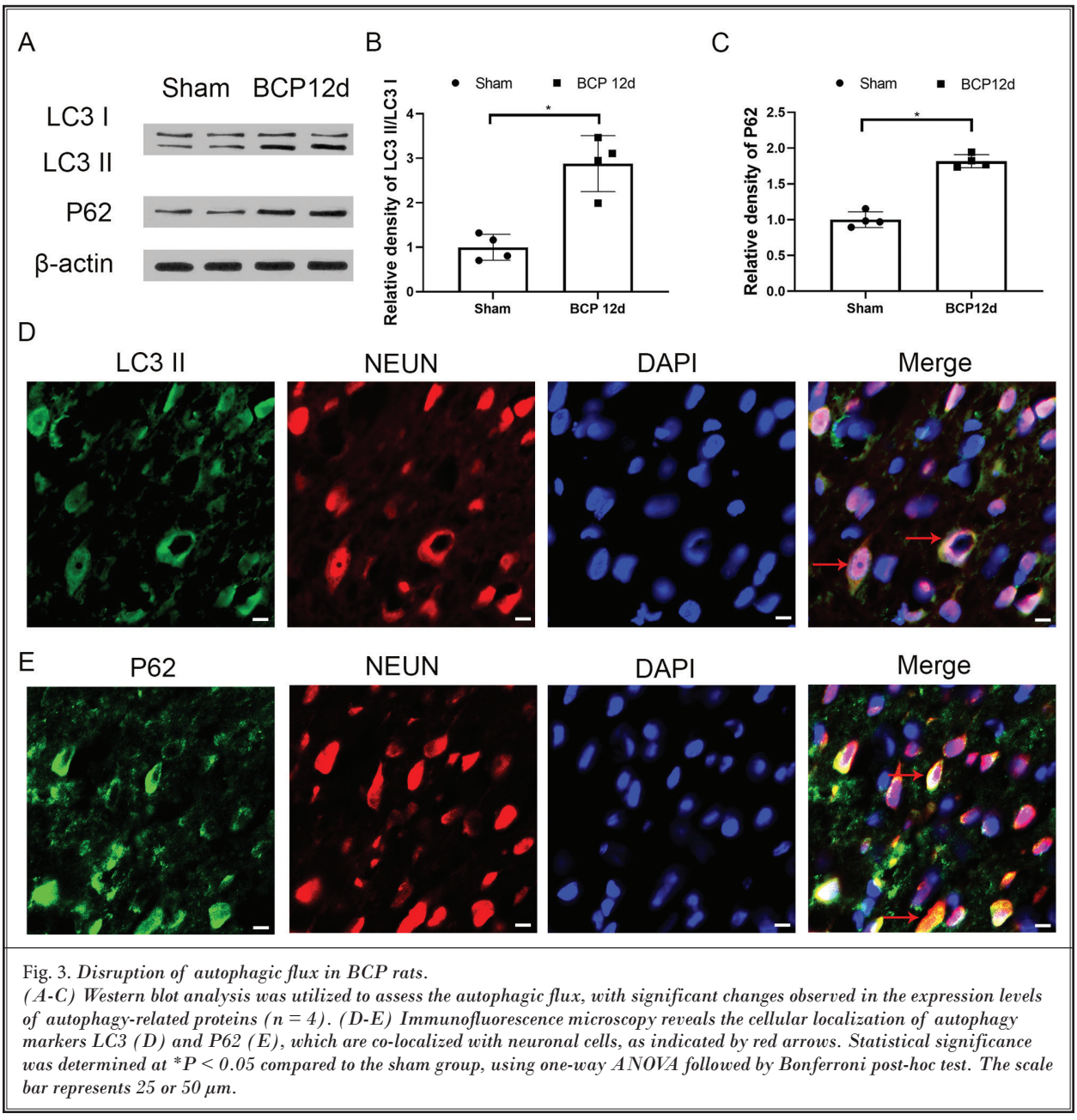

Fig. 3. *Disruption of autophagic flux in BCP rats.*
*(A-C) Western blot analysis was utilized to assess the autophagic flux, with significant changes observed in the expression levels of autophagy-related proteins (n = 4). (D-E) Immunofluorescence microscopy reveals the cellular localization of autophagy markers LC3 (D) and P62 (E), which are co-localized with neuronal cells, as indicated by red arrows. Statistical significance was determined at *P < 0.05 compared to the sham group, using one-way ANOVA followed by Bonferroni post-hoc test. The scale bar represents 25 or 50 μm.*

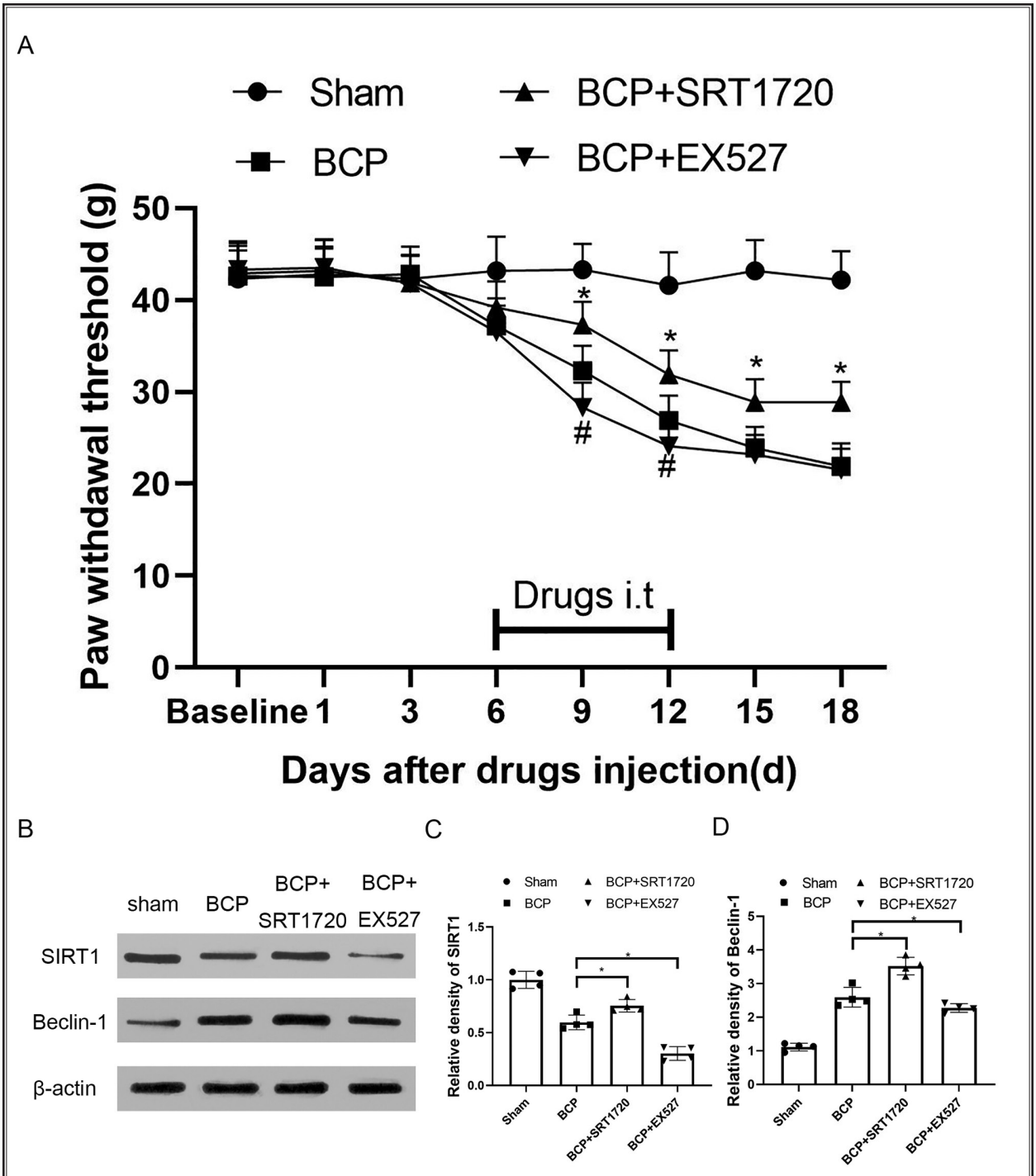

Fig. 4. *SIRT1 ameliorates nociceptive hypersensitivity in BCP rats.*
*(A) The impact of intrathecal SIRT1 agonists or inhibitors on the paw withdrawal threshold (PWT) for rats' hind paws (n = 8). (B-D) The influence of intrathecal SIRT1 agonists or inhibitors on the expression of spinal SIRT1 and Beclin-1, as detected by Western blot analysis (n = 4). Statistical significance is denoted by *P < 0.05 or #P < 0.05 when compared to the BCP group, using one-way ANOVA followed by a Bonferroni post-hoc test.*
Abbreviations: BCP, bone cancer pain; PWT, paw withdrawal threshold.

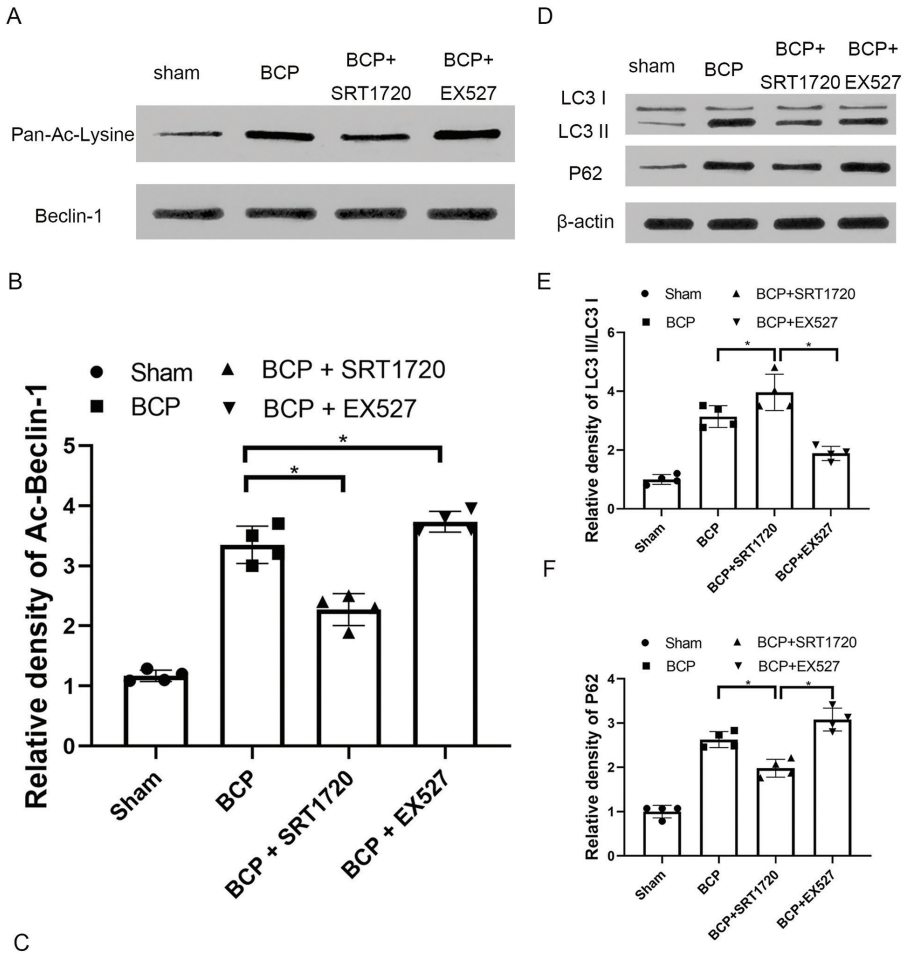

Fig. 5. *SIRT1 facilitates Beclin-1 nuclear translocation and restores autophagic flux. (A-B) The influence of SIRT1 on the expression levels of acetylated Beclin-1 in the spinal cord, as determined by Western blot analysis (n = 4). (C) The impact of SIRT1 on Beclin-1 nuclear translocation in spinal cord neurons, with red arrowheads indicating cytoplasmic Beclin-1 expression (n = 4). (D-F) Activation of SIRT1 enhances autophagic flux in the spinal cord, as evidenced by changes in autophagy markers (n = 4). *P < 0.05 indicates statistical significance compared to the BCP group, using one-way ANOVA followed by a Bonferroni post-hoc test.*

activation of SIRT1 in the dorsal horns of spinal cord tissues in rats with BCP can facilitate Beclin-1 nuclear translocation and restore autophagic flux.

SIRT1 Restores Autophagic Flux in Spinal Neuron

Next, this study used cell experiments to further verify the reparative effect of SIRT1 on neuronal autophagy flux. Immunofluorescence analysis in this study demonstrated that the expression levels of the autophagy marker LC3 were significantly higher in the SRT1720 agonist cell group than in the control group, with a statistically significant difference. Conversely, the expression of LC3 was significantly lower in the SRT1720+sirt1-siRNA cell group than in the SRT1720 agonist cell group, and this difference was also statistically significant. Additionally, the expression of LC3 was lower in the SRT1720+3-MA cell group than in the SRT1720 agonist cell group, and this difference was statistically significant as well (Figs. 6A-B). WB assays further revealed that the LC3II/LC3I ratio was significantly higher in the SRT1720 agonist cell group than in the control group, as was P62 expression. When compared to the SRT1720 agonist cell group, the LC3II/LC3I ratio was significantly lower in the SRT1720+sirt1-siRNA cell group, and P62 expression was significantly higher. Similarly, the SRT1720+3-MA cell group saw a significantly lower LC3II/LC3I ratio and significantly higher P62 expression (Figs. 6C-E).

These findings suggest that elevated SIRT1 expression in the neurons of the spinal cord dorsal horn may enhance the restoration of autophagic flux.

Discussion

BCP is a prevalent type of cancer-related pain for which effective treatment options remain elusive. BCP significantly diminishes cancer patients' quality of life, exacerbates the societal medical burden posed by the condition, and exerts an impact on patient prognoses. In this study, we elucidate the role of SIRT1 in spinal dorsal horn neurons in the context of BCP. Notably, we have demonstrated that SIRT1 facilitates Beclin-1 nuclear translocation to restore autophagic flux and investigated its potential mechanisms in mitigating the development of nociceptive hypersensitivity.

The findings of this study point at a reduction in SIRT1 expression and disruptions in autophagic flux within the spinal dorsal horn tissue in the context of BCP. This phenomenon appears to be neuron-specific, since it does not occur in astrocytes or microglia. Intrathecal administration of a SIRT1 agonist in a BCP rat model effectively reversed the downregulation of SIRT1, enhanced Beclin-1 nuclear translocation, stimulated autophagic flux, and consequently elevated the PWT in rats' hind paws. Cellular experiments further substantiated that SIRT1 could restore neuronal autophagic flux. These insights contribute significantly to our understanding of the SIRT1/autophagy signaling pathway's role in BCP.

Autophagy is a highly conserved intracellular degradation pathway that plays a crucial role in maintaining protein homeostasis, cellular survival, and development. Autophagy-related genes (ATGs) are instrumental in orchestrating the autophagy process by regulating major steps, including the expansion of autophagic membranes, the targeting of autophagic substrates, and the fusion of autophagosomes with lysosomes (28). Autophagosome formation is initiated by the ULK complex, which is responsible for generating phosphatidylinositol 3-phosphate (PI(3)P), a crucial lipid signaling molecule that operates at both the upstream and downstream levels of the phagocytic cell membrane (29). PI(3)P is synthesized by the PI3 kinase (PI3K) complex, comprising major components such as VPS34, VPS15, and Beclin-1 (30). Beclin-1, a pivotal regulator in autophagy, induces the formation of autophagic pre-structures, fosters the development of autophagic vacuoles, and influences various biological processes, including cellular metabolism, apoptosis, and autophagy itself (31). Post-translational modifications of Beclin-1 impact its stability, interactions, and capacity to regulate PI3K activity, thereby offering cells multiple mechanisms for modulating autophagy levels finely (32). LC3, a marker of the autophagic process, is integral to the formation of autophagic vesicles. At the onset of autophagy, LC3I is converted to LC3II, which facilitates the fusion of autophagosomes with lysosomes. During autophagy, P62 binds to ubiquitinated proteins and forms a complex with LC3II proteins on the inner membrane of autophagosomes, leading to their collective degradation within autophagic lysosomes (33,34). Studies across various pain models have indicated that an elevated LC3II/I ratio and increased P62 expression in the spinal cord dorsal horn, along with the restoration of autophagic flux, can ameliorate nociceptive hypersensitivity (35-37). In this study, an increased LC3II/I ratio was also observed in rats with BCP, as determined by WB analysis, suggesting a disruption in autophagic flux and an abnormal autophagosomal degradation process. Interestingly, an upregulation of Beclin-1 in

the spinal cord dorsal horn was also noted, implying the coexistence of enhanced autophagic activity with impaired autophagic flow in rats with BCP. The relationship between heightened autophagic activity and compromised autophagic flow in BCP merits further investigation.

In the WB analysis used in the present study, we observed a reduction in SIRT1 expression in the spinal cord dorsal horn tissue, with SIRT1 co-localizing with neurons. Immunofluorescence further revealed the co-localization of SIRT1 with Beclin-1. SIRT1, a nicotinamide adenine dinucleotide (NAD+)-dependent class III histone deacetylase, is known to remove acetyl groups from proteins, including Beclin-1, which is a key player in autophagy regulation. Acetylation, a significant post-translational modification, has been identified in thousands of proteins in mammalian cells, including Beclin-1 (38). This modification is a crucial regulatory mechanism that influences Beclin-1's function during autophagosome maturation, with expression levels of this protein being tied to the acetylation status of its lysine residues (32). Beclin-1 acetylation can suppress

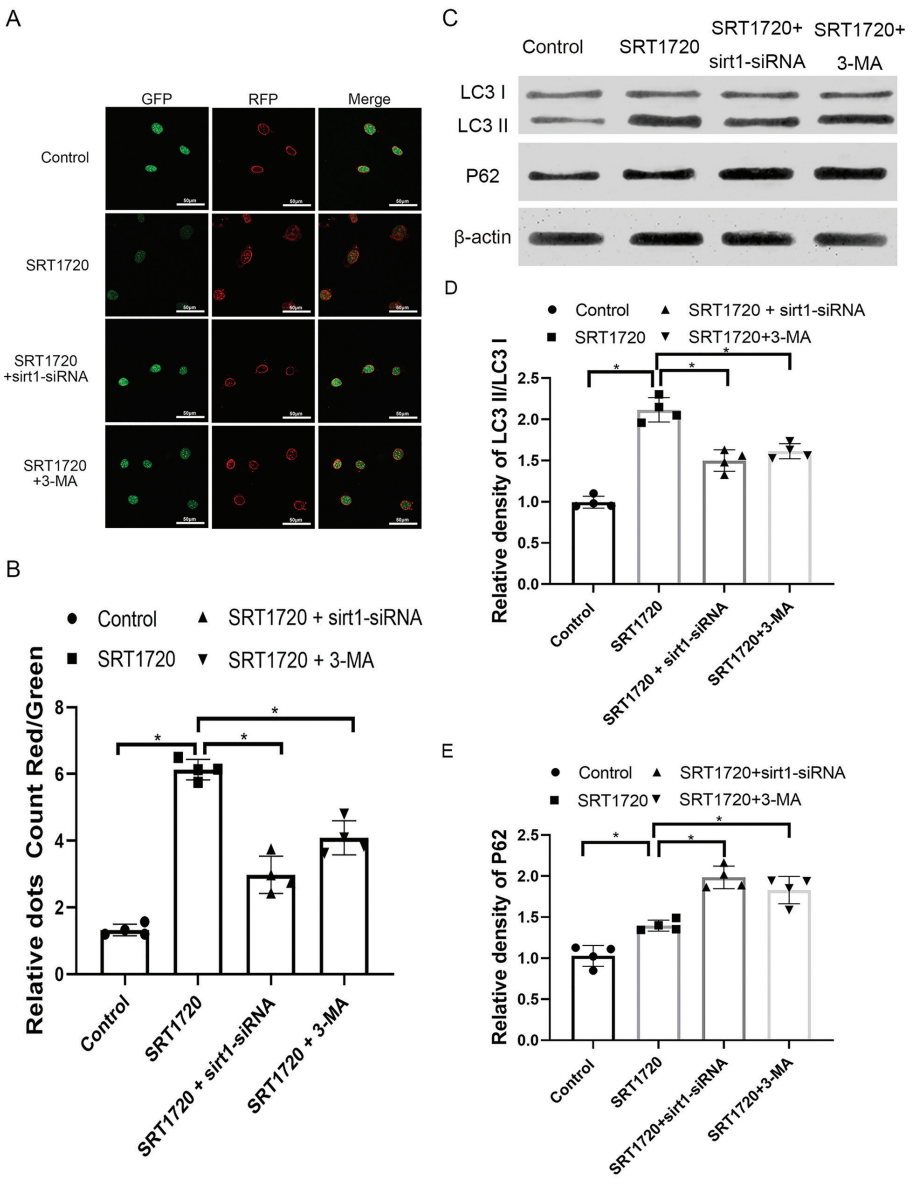

Fig. 6. *SIRT1-mediated activation of autophagic flux in spinal neurons. (A-B) Expression of LC3 in spinal neurons in response to SIRT1 activator SRT1720, a combination of SRT1720 and SIRT1 siRNA, or a combination of SRT1720 and the autophagy inhibitor 3-MA (n = 4). (C-E) Expression levels of autophagy-related proteins LC3 and P62 across 4 experimental groups. *P < 0.05 indicates statistical significance compared to the SRT1720 group, using 2-way ANOVA followed by a Bonferroni post-hoc test. The scale bar represents 50 μm.*

the autophagic response, while its deacetylation at lysine residues 430 and 437 by SIRT1 impacts autophagosome maturation and subsequent biological effects (39). These findings suggest that Beclin-1 may be a novel deacetylation target downstream of SIRT1, with SIRT1 potentially enhancing the autophagy pathway through the deacetylation of Beclin-1. Studies have shown that the nuclear translocation of beclin-1 promotes autophagosome formation and restores autophagic flux (16) and that intra-nuclear beclin-1 acetylation modification is a significant process that inhibits its nuclear translocation (38). Increased Beclin-1 expression and enhanced autophagic activity have been observed in various pain models, where the use of autophagy activators can alleviate nociceptive sensitization (19,36). For instance, a study found that SIRT1 agonists could mitigate the development of nociceptive hypersensitivity in rats (9,11). However, the role of SIRT1-promoted Beclin-1 nuclear translocation in pain development is not well understood. Our study explored the effects of intrathecal SIRT1 agonist injection on Beclin-1 nuclear translocation in a BCP model. Compared to the BCP group, the SIRT1 activator group showed further increases in Beclin-1 expression in the spinal cord dorsal horn tissue, decreases in acetylated Beclin-1, and increases in SIRT1 expression, along with an elevated pain threshold in BCP rats. In vitro experiments also demonstrated increased Beclin-1 nuclear translocation in spinal cord neurons after the injection of a SIRT1 activator. These results suggest that while autophagy initiation phase activity is enhanced in rats with BCP, increased acetylation of Beclin-1 may inhibit its nuclear translocation. The enhanced deacetylation of Beclin-1 after SIRT1 activation promotes Beclin-1 nuclear translocation, which may contribute to the alleviation of nociceptive sensitization in rats with BCP. Additionally, WB assays revealed that intrathecal injection of a SIRT1 activator increased the LC3II/I ratio, decreased P62, and restored autophagic flux in rats with BCP. Cellular experiments showed an increase in LC3II/I ratio and P62 expression when SIRT1 and 3-MA (an autophagy inhibitor) were used together, indicating that SIRT1's activation of autophagic flux could be blocked by autophagy inhibitors. This result is consistent with previous findings that autophagy inhibitors can prevent SIRT1 activation and relieve nociceptive hypersensitivity (22). However, when molecular changes in the spinal cord after the use of different pain models were compared, Beclin-1 was upregulated significantly after a chronic constriction injury (CCI), LC3-II was increased significantly after a spared nerve injury (SNI), and LC3-I and p62 levels were not significantly changed after an SNI or a CCI (40). This finding indicates that different types of pain induce distinct autophagy modulation patterns in the spinal dorsal horn, all of which can contribute to and perpetuate persistent pain.

Limitations

This study has several limitations that should be acknowledged. First, the study primarily focused on peripheral and spinal mechanisms of BCP, while supraspinal and cortical contributions (e.g., thalamus, anterior cingulate cortex) were not investigated. Additionally, pharmacological interventions were tested at only one time point, which might have prevented the results from reflecting the dynamic changes in pain sensitivity during tumor progression. Moreover, since this study was based on analyses of an animal model of BCP, high-quality clinical trials are still needed to further investigate the role of SIRT1 in BCP patients. Although these preclinical findings require validation in clinical populations, the consistency of SIRT1's effects across multiple pain assays strengthens its potential as both a therapeutic target and biomarker for BCP. Future studies should focus on correlating SIRT1 levels with pain scores in cancer patients' biopsies and developing SIRT1-targeting compounds with suitable pharmacokinetics for human use.

Conclusion

In summary, the findings of this study suggest that SIRT1 may be a therapeutic target molecule for BCP. Activating SIRT1 can alleviate pain hypersensitivity in rats with BCP, which may be related to the protein's role in restoring autophagic flux in spinal cord neurons. Notably, the deacetylation of Beclin-1 by SIRT1, promoting its nuclear translocation, may be a crucial step in the reconstruction of autophagic flux, which deserves further investigation. The results of this study provide new directions and ideas for the treatment of BCP.

Author Contributions

Qiuli He designed this study. Wenjie Li and Cuie Deng performed the study and statistical analyses. Zhiming Zhang prepared the tables and figures. Housheng Deng contributed to drafting the manuscript. All authors certify that they meet ICMJE authorship criteria, have reviewed the final version of the article, and agree to be accountable for all aspects of the work.

References

1. Philippe C, Rob C, Margherita P, et al. Bone metastasis: Mechanisms, therapies, and biomarkers. *Physiol Rev* 2020; 101:797-855.
2. Francesco M, Antonio C, Carmelo S, Paventi S, Tomei M, Bosco M. Cervical erector spinae plane block catheter in patient with severe clavicle pain caused by metastatic lung cancer. *Reg Anesth Pain Med* 2024; 50:528-530.
3. Zheng Z, Lv ZG, Lu M, Li H, Zhou J. Nerve-tumor crosstalk in tumor microenvironment: From tumor initiation and progression to clinical implications. *Biochim Biophys Acta Rev Cancer* 2024; 1879:189121.
4. Yu, T.Yumei, S.Zhen, X, et al.Altered gray matter volume and functional connectivity in lung cancer patients with bone metastasis pain. *J Neurosci Res* 2024:102
5. Zheng XQ, Wu YH, Huang JF, Wu AM. Neurophysiological mechanisms of cancer-induced bone pain. *J Adv Res* 2022; 35:117-127.
6. Romero-Morales P, Ruvalcaba-Paredes E, Garciadiego-Cázares D, et al. Neurophysiological mechanisms related to pain management in bone tumors. *Curr Neuropharmacol* 2020; 19:308-319.
7. Zhu X, Su Q, Xie H, et al. SIRT1 deacetylates WEE1 and sensitizes cancer cells to WEE1 inhibition. *Nat Chem Biol* 2023; 19:585-595.
8. Song FH, Liu DQ, Zhou YQ, Mei W. SIRT1: A promising therapeutic target for chronic pain. *CNS Neurosci Ther* 2022; 28:818-828.
9. Li MY, Ding JQ, Tang Q, et al. SIRT1 activation by SRT1720 attenuates bone cancer pain via preventing Drp1-mediated mitochondrial fission. *Biochim Biophys Acta Mol Basis Dis* 2019; 1865:587-598.
10. Yang C, Kang F, Wang S, Han M, Zhang Z, Li J. SIRT1 activation attenuates bone cancer pain by inhibiting mGluR1/5. *Cell Mol Neurobiol* 2019; 39:1165-1175.
11. Yang C, Kang F, Huang X, et al. Melatonin attenuates bone cancer pain via the SIRT1/HMGB1 pathway. *Neuropharmacology* 2022; 220:109254.
12. Ding Z, Du W, Huang J, et al. Allogeneic platelet lysate activates the SIRT1-PINK1/Parkin pathway: A promising approach for improving mitochondrial function in an in vitro model of intervertebral disc degeneration. *Int Immunopharmacol* 2025; 144:113700.
13. Li Y, An M, Fu X, et al. Bushen Wenyang Huayu Decoction inhibits autophagy by regulating the SIRT1-FoXO-1 pathway in endometriosis rats. *J Ethnopharmacol* 2023; 308:116277.
14. Mizushima N, Levine B. Autophagy in human diseases. *N Engl J Med* 2020; 383:1564-1576.
15. Fernández AF, Sebti S, Wei Y, et al. Author Correction: Disruption of the beclin 1-BCL2 autophagy regulatory complex promotes longevity in mice. *Nature* 2018; 561:E30.
16. Fernández AF, Sebti S, Wei Y, et al. Disruption of the beclin 1-BCL2 autophagy regulatory complex promotes longevity in mice. *Nature* 2018; 558:136-140.
17. Liu K, Shi Y, Guo X, et al. CHOP mediates ASPP2-induced autophagic apoptosis in hepatoma cells by releasing Beclin-1 from Bcl-2 and inducing nuclear translocation of Bcl-2. *Cell Death Dis* 2014; 5:e1323.
18. Yan Z, Liao H, Deng C, Zhong Y, Mayeesa TZ, Zhuo Y. DNA damage and repair in the visual center in the rhesus monkey model of glaucoma. *Exp Eye Res* 2022; 219:109031.
19. Tam TH, Zhang W, Tu Y, et al. Pain hypersensitivity is dependent on autophagy protein Beclin 1 in males but not females. *Cell Rep* 2024; 43:114293.
20. Wang Z, Xu H, Wang Z, et al. Traditional Chinese manual therapy (Tuina) improves knee osteoarthritis by regulating chondrocyte autophagy and apoptosis via the PI3K/AKT/mTOR pathway: An in vivo rat experiment and machine learning study. *J Inflamm Res* 2024; 17:6501-6519.
21. Li R, Shang J, Zhou W, Jiang L, Xie D, Tu G. Overexpression of HIPK2 attenuates spinal cord injury in rats by modulating apoptosis, oxidative stress, and inflammation. *Biomed Pharmacother* 2018; 103:127-134.
22. Gao S, Li N, Chen R, Su Y, Song Y, Liang S. Bushen Huoxue Formula modulates autophagic flux and inhibits apoptosis to protect nucleus pulposus cells by restoring the AMPK/SIRT1 pathway. *Biomed Res Int* 2022; 2022:8929448.
23. Hao C, Ma B, Gao N, Jin T, Liu X. Translocator protein (TSPO) alleviates neuropathic pain by activating spinal autophagy and nuclear SIRT1/PGC-1α signaling in a rat L5 SNL model. *J Pain Res* 2022; 15:767-778.
24. Ni H, Xu M, Kuang J, et al. Upregulation of LncRNA71132 in the spinal cord regulates hypersensitivity in a rat model of bone cancer pain. *Pain* 2022; 164:180-196.
25. Liu X, Zhu M, Ju Y, Li A, Sun X. Autophagy dysfunction in neuropathic pain. *Neuropeptides* 2019; 75:41-48.
26. Wei F, Wang Y, Yao J, et al. ZDHHC7-mediated S-palmitoylation of ATG16L1 facilitates LC3 lipidation and autophagosome formation. *Autophagy* 2024; 20:2719-2737.
27. Yao H, Li J, Liu Z, et al. Ablation of endothelial Atg7 inhibits ischemia-induced angiogenesis by upregulating Stat1 that suppresses Hif1a expression. *Autophagy* 2022; 19:1491-1511.
28. Shanlin R, Skulsuppaisarn M, Strong LM, et al. Three-step docking by WIPI2, ATG16L1, and ATG3 delivers LC3 to the phagophore. *Sci Adv* 2024; 10:eadj8027.
29. Wang J, An Z, Wu Z, et al. Spatial organization of PI3K-PI(3,4,5)P(3)-AKT signaling by focal adhesions. *Mol Cell* 2024; 84:4401-4418.e4409.
30. Yamamoto H, Matsui T. Molecular mechanisms of macroautophagy, microautophagy, and chaperone-mediated autophagy. *J Nippon Med Sch* 2024; 91:2-9.
31. Yu L, Chen Y, Tooze SA. Autophagy pathway: Cellular and molecular mechanisms. *Autophagy* 2018; 14:207-215.
32. Sun T, Li X, Zhang P, et al. Acetylation of Beclin 1 inhibits autophagosome maturation and promotes tumour growth. *Nat Commun* 2015; 6:7215.
33. Kung MH, Lin YS, Chang TH. Aichi virus 3C protease modulates LC3- and SQSTM1/p62-involved antiviral response. *Theranostics* 2020; 10:9200-9213.
34. Saito Y, Yako T, Otsu W, et al. A triterpenoid Nrf2 activator, RS9, promotes LC3-associated phagocytosis of photoreceptor outer segments in a p62-independent manner. *Free Radic Biol Med* 2020; 152:235-247.
35. Fu S, Sun H, Wang J, et al. Impaired neuronal macroautophagy in the prelimbic cortex contributes to comorbid anxiety-like behaviors in rats with chronic neuropathic pain. *Autophagy* 2024; 20:1559-1576.
36. Shao S, Xu CB, Chen CJ, et al. Divanillyl sulfone suppresses NLRP3 inflammasome activation via inducing mitophagy to ameliorate

chronic neuropathic pain in mice. *J Neuroinflammation* 2021; 18:142.

37. Wang D, Wei SN, Zhang L, et al. Impaired basal forebrain cholinergic neuron GDNF signaling contributes to perioperative sleep deprivation-induced chronicity of postsurgical pain in mice through regulating cholinergic neuronal activity, apoptosis, and autophagy. *CNS Neurosci Ther* 2024; 30:e70147.
38. Chen X, Pan Z, Fang Z, et al. Omega-3 polyunsaturated fatty acid attenuates traumatic brain injury-induced neuronal apoptosis by inducing autophagy through the upregulation of SIRT1-mediated deacetylation of Beclin-1. *J Neuroinflammation* 2018; 15:310.
39. Deng Z, Sun M, Wu J, et al. SIRT1 attenuates sepsis-induced acute kidney injury via Beclin1 deacetylation-mediated autophagy activation. *Cell Death Dis* 2021; 12:217.
40. Berliocchi L, Maiarù M, Varano GP, et al. Spinal autophagy is differently modulated in distinct mouse models of neuropathic pain. *Mol Pain* 2015; 11:3.